Rigid-body attitude tracking control under actuator faults and angular velocity constraints

Qiang Shen, *Member, IEEE,* Chengfei Yue, *Student Member, IEEE,* Cher Hiang Goh, *Senior Member, IEEE,* Baolin Wu, and Danwei Wang, *Senior Member, IEEE,*

***Abstract*—The problem of rigid-body attitude tracking is examined for the case that there exist actuator faults and angular velocity constraints during the attitude maneuver. With a hyperbolic tangent function as input signal, a first-order command filter is proposed to generate a virtual velocity error command for the angular velocity tracking error to follow. Then, an adaptive fault-tolerant controller based on the command filter is designed without requiring information of actuator fault, moment of inertia, and external disturbances. Through Lyapunov stability analysis, it is shown that the control law guarantees that the desired attitude is tracked even in the presence of actuator faults and external disturbances. Finally, simulations are conducted on a rigid spacecraft and results demonstrate the effectiveness of the proposed strategy.**

***Index Terms*—Fault-tolerant control, actuators, control allocation, model reference adaptive control, attitude tracking.**

I. INTRODUCTION

ATTITUDE tracking control of a rigid body is one of the most intensively studied topics in controls literature during the past decades, and a wide range of linear or nonlinear control solutions have been developed according to the application under consideration. For example, inverse optimal control [1], sliding mode control [2], H_∞ control [3], hybrid control [4], output feedback control [5], etc., have been proposed for solving the attitude tracking control problem. To design a controller with high control performance in practical situations, external disturbances, actuator faults, and angular velocity constraints are required to take into account. Therefore, the nonlinear attitude tracking controller should not only have fault-tolerant capability to handle actuator faults but also make the system satisfy angular rate constraints during the attitude maneuver. It is noted that adaptive sliding mode control technique is considered as an efficient way to cope with external disturbances and model uncertainties in nonlinear systems [6], [7], and has been widely applied in fault-tolerant control systems (FTCS) [8]–[11].

Q. Shen is with Temasek Laboratories, National University of Singapore, 117582 (e-mail: qiang.shen@hotmail.com).

C. Yue is with the Department of Electrical and Computer Engineering, National University of Singapore, Singapore 117582 (e-mail: chengfei_yue@u.nus.edu).

C. H. Goh is with the Department of Electrical and Computer Engineering, National University of Singapore, Singapore 117582, and also with DSO National Laboratories, Singapore 118230 (e-mail: elegch@nus.edu.sg).

B. Wu is with School of Astronautics, Harbin Institute of Technology, 150080, Harbin, People's Republic of China (e-mail: wubaolin@hit.edu.cn).

D. Wang is with the Department of Electrical and Electronic Engineering, Nanyang Technological University, Singapore 639798 (e-mail: edwwang@ntu.edu.sg).

To ensure the closed-loop system stability and acceptable control performance of the attitude tracking in the event of actuator faults, the design of fault tolerant control (FTC) has attracted increasing attention in recent years. Generally speaking, the existing fault-tolerant control (FTC) solutions can be categorized into two types: passive FTC and active FTC [12], [13]. Both passive and active FTC solutions have been developed for attitude control systems, and a comprehensive review can be found in [14]. As the stability is the number one consideration in a safety-critical system, a passive FTC approach with a simple control structure is always employed to ensure closed-loop stability with acceptable performance and make the overall system as insensitive as possible to a list of known faults. The authors of [15] presented an indirect adaptive robust controller to compensate the effects of the fault in attitude tracking systems. In [16], an adaptive fault-tolerant attitude tracking controller based on variable structure control was proposed for rigid spacecraft, where a dedicated parameter was introduced to adjust transient response of the closed-loop system. In [17], three fault-tolerant controllers were proposed to stabilize the attitude control system in finite time despite the existence of actuator faults, external disturbances, modelling uncertainties, and actuator saturation constraints. In comparison with the passive FTC approach, the active one requires a fault detection and diagnosis (FDD) scheme to attain the real-time fault information including the time instance that fault occurs, fault type, and fault size, and then the existing controller is reconfigured according to these online fault information such that an optimal or sub-optimal control solution with certain pre-set performance criteria can be maintained. In [18], sliding mode observer was designed to reconstruct the lumped fault including actuator fault and external disturbances in finite time, and a velocity-free attitude controller was synthesized to asymptotically stabilize the attitude. In [19], using integral sliding mode control technique, an active FTC strategy was developed to accommodate certain allowable actuator faults for the attitude control of a rigid spacecraft. In [20], a local fault identification approach was designed on each actuator to estimate the size of two different types of fault, and a finite-time reconfigurable controller with control allocation was developed to achieve attitude stabilization.

Another challenge in practical rigid-body attitude control is the constraint on angular rate. Due to the saturation limitation of low-rate gyro or mission specification requirement, the angular velocity should keep in the range of operation. In [21], a cascade PD controller was developed for spacecraft eigenaxis rotation with consideration of angular velocity and control torque constraints. This controller was commonly used in practical attitude control systems, but it was not easy to compute the controller gains and prove the closed-loop system's stability rigorously. In [22], an adaptive attitude controller based on the backstepping technique was proposed, where the angular velocity was guaranteed to operate within a given domain by constructing a barrier Lyapunov function. In [23], a time efficient attitude maneuver strategy was designed for a rigid spacecraft via braking curve design and sliding mode control, where L_∞ torque allocation method was proposed to determine the rigid body's angular rate and acceleration limits. With the use of the neural network approximation and virtual angular velocity command from a hyperbolic tangent function, an adaptive controller was designed for rigid-body attitude stabilization with consideration of assigned control saturation limits and angular rate constraints [24]. However, none of these aforementioned literatures have the capability to deal with actuator faults simultaneously along with angular velocity limits.

This paper investigates the FTC design for attitude tracking systems of a rigid body in the presence of actuator faults, angular velocity constraints, and external disturbances. A command filter with bounded input is firstly used to generate a magnitude limited virtual velocity error trajectory for the angular velocity tracking error to follow. One of the key features of the command filter is that a safety scale is introduced to provide a saturation margin so that the angular velocity constraint could not be violated effortlessly. Through limiting the magnitude of the attitude tracking error, constraints on the angular velocity can be ensured consequently. Then, we propose a command filter-based adaptive controller, which not only compensates the effects of actuator faults and external disturbances collectively without the need for FDD, but also makes the angular velocity error track the virtual velocity trajectory asymptotically. The uniform ultimate boundedness of the closed-loop signals is ensured by the Lyapunov direct approach. The effectiveness of the proposed FTC method is demonstrated in a spacecraft attitude tracking system subject to loss of actuator effectiveness and angular rate limitations.

The remainder of this paper is organized as follows. In Section II, the mathematic models for rigid-body attitude tracking systems and actuator faults are presented, and control problem formulation is summarized. Section III presents the command filter and derives the fault-tolerant controller. In Section IV illustrates the application of the control strategy to a rigid spacecraft, followed by conclusions in Section V.

II. System Description and Problem Statement

A. Rigid-body Attitude Dynamics

The kinetics equation for the attitude motion of a rigid body takes the form [25]

$$\boldsymbol{J}\dot{\boldsymbol{\omega}} = -\boldsymbol{\omega}^\times \boldsymbol{J}\boldsymbol{\omega} + \boldsymbol{u} + \boldsymbol{d}, \tag{1}$$

where $\boldsymbol{J} \in \mathbb{R}^{3\times 3}$ denotes the inertia matrix of the rigid body and is symmetric positive-definite, $\boldsymbol{u} \in \mathbb{R}^3$ denotes the control torque produced by three actuators that are aligned with the principle axes of inertia, $\boldsymbol{\omega} \in \mathbb{R}^3$ is the angular velocity vector in a body-fixed frame with respect to inertial frame, $\boldsymbol{d} \in \mathbb{R}^3$ denotes external disturbances, and $\boldsymbol{a}^\times \in \mathbb{R}^{3\times 3}$ denotes the skew-symmetric matrix for a column vector $\boldsymbol{a} \in \mathbb{R}^3$.

The kinematics in terms of quaternion obey the differential equation [26]

$$\begin{cases} \dot{\boldsymbol{q}} = \frac{1}{2}(\boldsymbol{q}^\times + q_0 \boldsymbol{I}_3)\boldsymbol{\omega} \\ \dot{q}_0 = -\frac{1}{2}\boldsymbol{q}^T\boldsymbol{\omega}, \end{cases} \tag{2}$$

where $\boldsymbol{Q} = [q_1\ q_2\ q_3\ q_0]^T = [\boldsymbol{q}^T\ q_0]^T \in \mathbb{R}^3 \times \mathbb{R}$ is the unit-quaternion in the body-fixed frame with respect to the inertia frame, $\boldsymbol{I}_3 \in \mathbb{R}^{3\times 3}$ is the 3×3 identity matrix. Here, it is noted that the unit-quaternion $\boldsymbol{Q}$ satisfies the identical relation $q_0^2 + \boldsymbol{q}^T\boldsymbol{q} = 1$.

In this paper, two different types of actuator faults that are categorized by the way faults enter to the system are taken into account, namely multiplicative fault and additive bias fault [27]. The actuator fault model is described as [17], [28]

$$\boldsymbol{u} = \boldsymbol{E}\boldsymbol{u}_c + \boldsymbol{f}_a, \tag{3}$$

where $\boldsymbol{u}_c = [u_{c1}\ u_{c2}\ u_{c3}]^T \in \mathbb{R}^3$ is commanded or desired control torque computed by the controller, the diagonal matrix $\boldsymbol{E} = \mathrm{diag}\{e_1, e_2, e_3\} \in \mathbb{R}^{3\times 3}$ is employed to describe the effectiveness of the actuators and its diagonal elements are constrained between 0 and 1, that is $0 < e_i \leq 1, i \in \{1,2,3\}$. Noting that we only consider healthy condition ($e_i = 1$) and partial loss of effectiveness faults ($0 < e_i < 1$) in the actuator fault model, and the case of total failure ($e_i = 0$) is not considered as there is no actuator redundancy. The variable $\boldsymbol{f}_a = [f_{a1}\ f_{a2}\ f_{a3}]^T \in \mathbb{R}^3$ represents the additive bias fault.

Substituting the actuator fault model (3) into the kinetics equation (1), the attitude dynamics in the presence of actuator faults can be described as

$$\boldsymbol{J}\dot{\boldsymbol{\omega}} = -\boldsymbol{\omega}^\times \boldsymbol{J}\boldsymbol{\omega} + \boldsymbol{E}\boldsymbol{u}_c + \boldsymbol{f}_a + \boldsymbol{d}. \tag{4}$$

B. Attitude Error Dynamics

Suppose the desired attitude of the rigid body is denoted as $\boldsymbol{Q}_d = [\boldsymbol{q}_d^T\ q_{d0}]^T$ in the body-fixed frame and also constructed to satisfy $\|\boldsymbol{q}_d\|^2 + {q_{d0}}^2 = 1$. To describe the discrepancy between the desired attitude $\boldsymbol{Q}_d$ and current attitude $\boldsymbol{Q}$, another unit quaternion $\boldsymbol{Q}_e$ known as the attitude tracking error is also introduced as [29]

$$\boldsymbol{Q}_e = \boldsymbol{Q}_d^{-1} \otimes \boldsymbol{Q} = \begin{bmatrix} q_{d0}\boldsymbol{q} + q_0\boldsymbol{q}_d + \boldsymbol{q}_d^\times \boldsymbol{q} \\ q_{d0}q_0 - \boldsymbol{q}_d^T\boldsymbol{q} \end{bmatrix}. \tag{5}$$

where $\boldsymbol{Q}_d^{-1}$ is the inverse or conjugate of the desired quaternion given by $\boldsymbol{Q}_d^{-1} = [-\boldsymbol{q}_d^T\ q_{d0}]^T$, and $\otimes$ represents the quaternion multiplication operator for unit quaternion $\boldsymbol{Q}$ and $\boldsymbol{Q}_e$. Next, we assume that the desired angular velocity is $\boldsymbol{\omega}_d$ that is related the desired attitude in the desired body-fixed frame. Consequently, the angular velocity error $\boldsymbol{\omega}_e$ is computed as [30]

$$\boldsymbol{\omega}_e = \boldsymbol{\omega} - \boldsymbol{C}\boldsymbol{\omega}_d, \tag{6}$$

where $\boldsymbol{C}$ is the rotation matrix defined as $\boldsymbol{C} = (q_{e0}^2 - \boldsymbol{q}_e^T\boldsymbol{q}_e)\boldsymbol{I}_3 + 2\boldsymbol{q}_e\boldsymbol{q}_e^T - 2q_{e0}\boldsymbol{q}_e^\times$. Note that the rotation matrix $\boldsymbol{C} \in SO(3) = \{\boldsymbol{C} \in \mathbb{R}^{3\times 3} : \boldsymbol{C}^T\boldsymbol{C} = \boldsymbol{C}\boldsymbol{C}^T = \boldsymbol{I}_3, \det(\boldsymbol{C}) =$

$1\}$ [4]. Now, in view of quaternion error equation in (5) and angular velocity error in (6), the attitude tracking error dynamics with consideration of actuator faults is derived as

$$\begin{cases} \boldsymbol{J}\dot{\boldsymbol{\omega}}_e = -\boldsymbol{\omega}^{\times}\boldsymbol{J}\boldsymbol{\omega} + \boldsymbol{E}\boldsymbol{u}_c + \boldsymbol{f}_a + \boldsymbol{d} \\ \qquad\quad +\boldsymbol{J}(\boldsymbol{\omega}_e^{\times}\boldsymbol{C}\boldsymbol{\omega}_d - \boldsymbol{C}\dot{\boldsymbol{\omega}}_d) \\ \dot{\boldsymbol{q}}_e = \frac{1}{2}(\boldsymbol{q}_e^{\times} + q_{e0}\boldsymbol{I}_3)\boldsymbol{\omega}_e \\ \dot{q}_{e0} = -\frac{1}{2}\boldsymbol{q}_e^T\boldsymbol{\omega}_e. \end{cases} \tag{7}$$

To proceed, the following assumptions are in order.

Assumption 1: The desired angular velocity of rigid-body and its time derivative are bounded such that $\|\boldsymbol{\omega}_d\| \leq \omega_{d,max} < \infty$ and $\|\dot{\boldsymbol{\omega}}_d\| \leq \bar{\omega}_{d,max} < \infty$, in which $\omega_{d,max}$ and $\bar{\omega}_{d,max}$ are positive constants.

Assumption 2: The external disturbance $\boldsymbol{d}$ is bounded such that $\|\boldsymbol{d}\| \leq d_{\max}$, where $d_{\max}$ is an unknown positive constant, and the notation $\|\cdot\|$ denotes the Euclidean norm or its induced norm.

Assumption 3: The inertia matrix $\boldsymbol{J}$ is a symmetric, positive definite and bounded constant matrix. There exists a positive constant $J_{\max}$ such that $\boldsymbol{x}^T\boldsymbol{J}\boldsymbol{x} \leq J_{\max}\|\boldsymbol{x}\|^2$ for any $\boldsymbol{x} \in \mathbb{R}^3$.

Assumption 4: The actuator effectiveness matrix $\boldsymbol{E}$ and additive fault $\bar{\boldsymbol{u}}$ are unknown, possibly fast time-varying and unpredictable, but bounded in some unknown constants $e_{\min}$ and $f_{\max}$ such that $0 < e_{\min} \leq \|\boldsymbol{E}\| \leq 1$ and $\|\bar{\boldsymbol{u}}\| \leq f_{\max}$.

Remark 1: Assumptions 1-3 are commonly found in most existing works focusing on attitude tracking problems, for example [1], [2]. Assumption 4 guarantees that the attitude tracking system subject to actuator faults is still controllable and three-axis attitude tracking can be achieved. Similar assumption can also be found in [27]. In addition, note that it would be difficult to get the exact values of bounds on external disturbances, inertia matrix, and actuator faults involved in Assumptions 2-4 even though the fact that those bounds do exist in practice. Therefore, the developed attitude tracking controller should be independent of those bound information.

C. Problem Statement

Suppose that all the status are available, and the angular velocity constraint is given by

$$\boldsymbol{\omega} \in D_{\omega} = \{|\omega_i(t)| \leq \omega_{\max}, \quad i = 1,2,3\}, \tag{8}$$

where $\omega_{\max}$ is the limited operating angular rate.

For attitude tracking systems, instead of attitude and angular velocity, their tracking errors are utilized in controller design. In this case, it would be easier and more institutive to limit the angular velocity tracking error rather than angular velocity itself when angular velocity is taken into consideration. In light of this consideration, the attitude constraint is satisfied through limiting the magnitude of angular velocity tracking error. Suppose that the angular velocity tracking error constrains are formulated as

$$\boldsymbol{\omega}_e \in D_{\omega_e} = \{|\omega_{e,i}(t)| \leq \omega_{e,\max}, \quad i = 1,2,3\}, \tag{9}$$

where $\omega_{e,\max}$ is a constant representing the maximal magnitude of ω_e. In view of (6), $\|\boldsymbol{C}\| = 1$, and Assumption 1, if $\omega_{e,\max}$ is selected as

$$\omega_{e,\max} = \omega_{\max} - \omega_{d,\max}, \tag{10}$$

then it is clear that the angular velocity constraint in (8) is also ensured.

Therefore, the objective of this paper is stated as follows: Consider the rigid-body attitude tracking system described in (7) with consideration of disturbances and actuator faults, for any given initial attitude orientation and initial angular velocity $\boldsymbol{\omega}(0) \in D_{\omega}$, design a command filter-based fault-tolerant controller to not only achieve stable attitude tracking, but also satisfy angular rate tracking error constraint in (9) during the attitude maneuver.

III. Controller Design and Stability Analysis

In this section, the main result dealing with attitude tracking of a rigid body under actuator faults and angular rate constraints is presented. A command filter using a hyperbolic tangent function as input signal is designed firstly. Sequentially, we propose an adaptive fault-tolerant controller based on the command filter to achieve stable attitude tracking and against actuator faults for the rigid-body attitude tracking system.

A. Command Filter Design

The purpose of the command filter is to generate a trajectory defined as virtual angular velocity error $\boldsymbol{\omega}_v$ for the true angular velocity tracking error $\boldsymbol{\omega}_e$ to follow. The virtual angular velocity error command $\boldsymbol{\omega}_v$ is introduced based on the following command filter:

$$T_0\dot{\boldsymbol{\omega}}_v + \boldsymbol{\omega}_v = \alpha\boldsymbol{\omega}_v^0, \tag{11}$$

where T_0 is the time constant, the constant α denotes a safety scale satisfying $0 < \alpha \leq 1$, and $\boldsymbol{\omega}_v^0$ is the input of the command filter given by

$$\boldsymbol{\omega}_v^0 = -\omega_{e,\max}\tanh(c\boldsymbol{q}_e) \tag{12}$$

with $\boldsymbol{\omega}_v(0) = \boldsymbol{\omega}_v^0(0)$. From (12) and command filter defined in (11), it is easy to verify that

$$\|\boldsymbol{\omega}_v^0\| \leq \omega_{e,\max} \text{ and } \|\boldsymbol{\omega}_v\| \leq \alpha\omega_{e,\max}. \tag{13}$$

According to (12), the input $\boldsymbol{\omega}_v^0$ to the commander filter is a hyperbolic tangent function in terms of attitude tracking error $\boldsymbol{q}_e$, which implies that the command filter builds up a mapping between attitude tracking error $\boldsymbol{q}_e$ and virtual angular velocity error command $\boldsymbol{\omega}_v$. It is noted that $\boldsymbol{\omega}_v^0$ goes to zero along with the convergence of $\boldsymbol{q}_e$. If the input of command filter becomes zero, it is clear from (11) that $\boldsymbol{\omega}_v$ converges to zero ultimately. Since $\boldsymbol{\omega}_v$ determines a desired trajectory for angular velocity tracking error $\boldsymbol{\omega}_e$, $\boldsymbol{\omega}_e$ also goes to zero ultimately as long as $\boldsymbol{\omega}_e$ tracks $\boldsymbol{\omega}_v$ successfully, which will be ensured using the proposed controller in the following. Moreover, if $\boldsymbol{\omega}_e$ follows its virtual desired trajectory $\boldsymbol{\omega}_v$, the magnitude of $\boldsymbol{\omega}_e$ is also bounded as $\|\boldsymbol{\omega}_e\| \leq \alpha\omega_{e,\max}$ due to the boundedness of $\boldsymbol{\omega}_v$ shown in (13). As the safety scale is between 0 and 1, it is clear that the angular velocity error constraints in (9) is satisfied.

Here, it should also be noted that the safety scale α provides a saturation margin for the angular velocity and guarantees that the actual velocity will not exceed its allowable maximum despite the tracking error, especially in the initial phase where the tracking error is very large.

Property 1 [24]: For any constant $x \in (-1 \quad 1)$, according to the definition of hyperbolic tangent function, there is a constant c_0 such that the following equation was established:

$$x^2 \leq x \tanh(cx), \qquad \forall\, c \geq c_0. \tag{14}$$

B. Fault-Tolerant Attitude Tracking Controller

To facilitate the attitude tracking controller and subsequent analysis, another two errors, denoted by virtual tracking error $\boldsymbol{\omega}_a \in \mathbb{R}^3$ and command filter error $\boldsymbol{\omega}_f \in \mathbb{R}^3$, are also defined as

$$\boldsymbol{\omega}_a = \boldsymbol{\omega}_e - \boldsymbol{\omega}_v, \tag{15}$$

$$\boldsymbol{\omega}_f = \boldsymbol{\omega}_v - \alpha\boldsymbol{\omega}_v^0. \tag{16}$$

The virtual tracking error $\boldsymbol{\omega}_a$ describes the discrepancy between angular velocity tracking error and its virtual command produced by command filter, while the command filter error $\boldsymbol{\omega}_f$ is the difference between virtual command and command filter input. According to (13) and (6), the fact $\|\boldsymbol{C}\| = 1$, and Assumption 1, it is clear from (16) that $\boldsymbol{\omega}_a$ and $\boldsymbol{\omega}_f$ are respectively bounded by

$$\|\boldsymbol{\omega}_a\| \leq \|\boldsymbol{\omega} - \boldsymbol{C}\boldsymbol{\omega}_d - \boldsymbol{\omega}_v\| \leq \|\boldsymbol{\omega}\| + \omega_{d,\max} + \alpha\omega_{e,\max} \tag{17}$$

and

$$\|\boldsymbol{\omega}_f\| \leq \|\boldsymbol{\omega}_v - \alpha\boldsymbol{\omega}_v^0\| \leq 2\alpha\omega_{e,\max}\,. \tag{18}$$

From (16), the dynamic equation for $\boldsymbol{\omega}_a$ left multiplied by inertia matrix is determined as

$$\begin{aligned}\boldsymbol{J}\dot{\boldsymbol{\omega}}_a =& \boldsymbol{J}\dot{\boldsymbol{\omega}}_e - \boldsymbol{J}\dot{\boldsymbol{\omega}}_v \\ =& -\boldsymbol{\omega}^\times\boldsymbol{J}\boldsymbol{\omega} + \boldsymbol{E}\boldsymbol{u}_c + \boldsymbol{f}_a + \boldsymbol{d} \\ &+ \boldsymbol{J}(\boldsymbol{\omega}_e^\times\boldsymbol{C}\boldsymbol{\omega}_d - \boldsymbol{C}\dot{\boldsymbol{\omega}}_d) - \frac{1}{T_0}\boldsymbol{J}\boldsymbol{\omega}_f.\end{aligned} \tag{19}$$

In addition, taking the time derivative of $\boldsymbol{\omega}_f$, it founds that

$$\dot{\boldsymbol{\omega}}_f = \dot{\boldsymbol{\omega}}_v - \alpha\dot{\boldsymbol{\omega}}_v^0 = -\frac{\boldsymbol{\omega}_f}{T_0} - \alpha\dot{\boldsymbol{\omega}}_v^0 \tag{20}$$

According to (20), it is obtained that

$$\begin{aligned}\boldsymbol{\omega}_f^T\dot{\boldsymbol{\omega}}_f =& -\frac{\boldsymbol{\omega}_f^T\boldsymbol{\omega}_f}{T_0} - \alpha\boldsymbol{\omega}_f^T\dot{\boldsymbol{\omega}}_v^0 \\ \leq& -\frac{\boldsymbol{\omega}_f^T\boldsymbol{\omega}_f}{T_0} + c\alpha\omega_{e,\max}\|\boldsymbol{\omega}_f\|\|\dot{\boldsymbol{q}}_e\|,\end{aligned} \tag{21}$$

where the fact that

$$\frac{\mathrm{d}}{\mathrm{d}t}\tanh(x) = \frac{1}{\cosh^2(x)}\dot{x}, \quad \forall\, x(t) \in \mathbb{R} \tag{22}$$

with

$$\frac{1}{\cosh^2(x)} \leq 1, \quad \forall\, x(t) \in \mathbb{R} \tag{23}$$

is used. Then, based on attitude error kinematics in (4) and the fact $\|\boldsymbol{q}_e^\times + q_{e0}\boldsymbol{I}_3\| \leq 1$, the inequality (21) is rewritten as

$$\begin{aligned}\boldsymbol{\omega}_f^T\dot{\boldsymbol{\omega}}_f \leq& -\frac{\boldsymbol{\omega}_f^T\boldsymbol{\omega}_f}{T_0} + \frac{c\alpha\omega_{e,\max}}{2}\|\boldsymbol{\omega}_f\|\|\boldsymbol{q}_e^\times + q_{e0}\boldsymbol{I}_3\|\|\boldsymbol{\omega}_e\| \\ \leq& -\left(\frac{1}{T_0} - \frac{c\alpha\omega_{e,\max}(g_1+g_2)}{4}\right)\boldsymbol{\omega}_f^T\boldsymbol{\omega}_f \\ &+ \frac{c\alpha\omega_{e,\max}}{4g_1}\boldsymbol{\omega}_a^T\boldsymbol{\omega}_a + \frac{c\alpha\omega_{e,\max}}{4g_2}\boldsymbol{\omega}_v^T\boldsymbol{\omega}_v,\end{aligned} \tag{24}$$

where g_1 and g_2 are two small constants, and Young's inequality is used.

Define a continuous positive definite function V_1 as

$$V_1 = \lambda\left[\boldsymbol{q}_e^T\boldsymbol{q}_e + (1-q_{e0})^2\right] + \frac{1}{2}\boldsymbol{\omega}_a^T\boldsymbol{J}\boldsymbol{\omega}_a + \frac{1}{2}\boldsymbol{\omega}_f^T\boldsymbol{\omega}_f, \tag{25}$$

where λ is a positive constant. Taking the time derivative of V_1 yields

$$\begin{aligned}\dot{V}_1 =& \lambda\boldsymbol{q}_e^T\boldsymbol{\omega}_e + \boldsymbol{\omega}_a^T\boldsymbol{J}\dot{\boldsymbol{\omega}}_a + \boldsymbol{\omega}_f^T\dot{\boldsymbol{\omega}}_f \\ \leq& -\lambda\left(\alpha\omega_{e,\max} - \frac{\gamma}{2}\right)\boldsymbol{q}_e^T\boldsymbol{q}_e + \frac{\lambda}{2\gamma}\boldsymbol{\omega}_f^T\boldsymbol{\omega}_f + \boldsymbol{\omega}_f^T\dot{\boldsymbol{\omega}}_f \\ &+ \boldsymbol{\omega}_a^T\Bigg[-\boldsymbol{\omega}^\times\boldsymbol{J}\boldsymbol{\omega} + \boldsymbol{E}\boldsymbol{u}_c + \boldsymbol{f}_a + \boldsymbol{d} - \frac{1}{T_0}\boldsymbol{J}\boldsymbol{\omega}_f \\ &+ \boldsymbol{J}(\boldsymbol{\omega}_e^\times\boldsymbol{C}\boldsymbol{\omega}_d - \boldsymbol{C}\dot{\boldsymbol{\omega}}_d) + \lambda\boldsymbol{q}_e\Bigg],\end{aligned} \tag{26}$$

where the Property 1 is used and γ is a small constant. Using inequality (24), we have

$$\begin{aligned}\dot{V}_1 \leq& -\lambda\left(\alpha\omega_{e,\max} - \frac{\gamma}{2}\right)\boldsymbol{q}_e^T\boldsymbol{q}_e \\ &-\left(\frac{1}{T_0} - \frac{c\alpha\omega_{e,\max}(g_1+g_2)}{4} - \frac{\lambda}{2\gamma}\right)\boldsymbol{\omega}_f^T\boldsymbol{\omega}_f \\ &+ \boldsymbol{\omega}_a^T\boldsymbol{\Theta} + \boldsymbol{\omega}_a^T\boldsymbol{E}\boldsymbol{u}_c + \frac{c\alpha\omega_{e,\max}}{4g_2}\boldsymbol{\omega}_v^T\boldsymbol{\omega}_v,\end{aligned} \tag{27}$$

where the variable $\boldsymbol{\Theta}$ is given by

$$\begin{aligned}\boldsymbol{\Theta} =& -\boldsymbol{\omega}^\times\boldsymbol{J}\boldsymbol{\omega} + \boldsymbol{f}_a + \boldsymbol{d} - \frac{1}{T_0}\boldsymbol{J}\boldsymbol{\omega}_f \\ &+ \boldsymbol{J}(\boldsymbol{\omega}_e^\times\boldsymbol{C}\boldsymbol{\omega}_d - \boldsymbol{C}\dot{\boldsymbol{\omega}}_d) + \lambda\boldsymbol{q}_e + \frac{c\alpha\omega_{e,\max}}{4g_1}\boldsymbol{\omega}_a.\end{aligned} \tag{28}$$

In view of Assumptions 1-4 and equalities in (17) and (18), we obtain the following inequalities

$$\begin{aligned}&\|-\boldsymbol{\omega}^\times\boldsymbol{J}\boldsymbol{\omega}\| \leq J_{\max}\|\boldsymbol{\omega}\|^2, \\ &\left\|\boldsymbol{J}\boldsymbol{\omega}_e^\times\boldsymbol{C}\boldsymbol{\omega}_d + \frac{c\alpha\omega_{e,\max}}{4g_1}\boldsymbol{\omega}_a\right\| \\ &\leq \left(J_{\max}\omega_{d,\max} + \frac{c\alpha\omega_{e,\max}}{4g_1}\right)\|\boldsymbol{\omega}\| \\ &\quad + J_{\max}\omega_{d,\max}^2 + \frac{c\alpha}{4g_1}\omega_{e,\max}\omega_{d,\max} + \frac{c\alpha^2}{4g_1}\omega_{e,\max}^2, \\ &\left\|\boldsymbol{f}_a + \boldsymbol{d} - \frac{1}{T_0}\boldsymbol{J}\boldsymbol{\omega}_f - \boldsymbol{J}\boldsymbol{C}\dot{\boldsymbol{\omega}}_d + \lambda\boldsymbol{q}_e\right\| \\ &\leq f_{\max} + d_{\max} + J_{\max}\bar{\omega}_{d,\max} + \frac{2\alpha\omega_{e,\max}J_{\max}}{T_0} + \lambda,\end{aligned}$$

which show that $\boldsymbol{\Theta}$ is bounded by a polynomial function of $\boldsymbol{\omega}$. More specifically, there exists a unknown constant $b > 0$ such that

$$\|\boldsymbol{\Theta}\| \leq b\psi(\cdot), \tag{29}$$

where

$$\begin{aligned}b = \max\Bigg\{& J_{\max}, J_{\max}\omega_{d,\max} + \frac{c\alpha\omega_{e,\max}}{4g_1}, \\ & J_{\max}\left(\omega_{d,\max}^2 + \bar{\omega}_{d,\max} + \frac{2\alpha\omega_{e,\max}}{T_0}\right) + f_{\max} \\ &+ \frac{c\alpha}{4g_1}\left(\omega_{e,\max}\omega_{d,\max} + \alpha\omega_{e,\max}^2\right) + d_{\max} + \lambda\Bigg\}\end{aligned} \tag{30}$$

and

$$\psi(\cdot) = \|\boldsymbol{\omega}\|^2 + \|\boldsymbol{\omega}\| + 1. \tag{31}$$

Therefore, we rewrite the inequality (27) as

$$\begin{aligned}\dot{V}_1 \leq & -\lambda\left(\alpha\omega_{e,\max} - \frac{\gamma}{2}\right)\boldsymbol{q}_e^T\boldsymbol{q}_e - \eta\boldsymbol{\omega}_f^T\boldsymbol{\omega}_f \\ & + b\psi(\cdot)\|\boldsymbol{\omega}_a\| + \boldsymbol{\omega}_a^T\boldsymbol{E}\boldsymbol{u}_c + \frac{c\alpha^3}{4g_2}\omega_{e,\max}^3,\end{aligned} \tag{32}$$

where $\eta = \frac{1}{T_0} - \frac{c\alpha\omega_{e,\max}(g_1+g_2)}{4} - \frac{\lambda}{2\gamma}$ is a constant scale. Noting that b is an unknown (bearing no physical meaning) parameter, the term $b\psi(\cdot)\|\boldsymbol{\omega}_a\|$ in the foregoing inequality cannot be compensated from controller directly. To relax the requirement of the parameter b in controller, an adaptive estimator is constructed as

$$\dot{\hat{b}} = -\sigma\varrho\hat{b} + \frac{\sigma\psi^2(\cdot)\|\boldsymbol{\omega}_a\|^2}{\psi(\cdot)\|\boldsymbol{\omega}_a\| + \iota} \tag{33}$$

where $\hat{b}$ is the estimation of the unknown constant b, σ and ϱ are positive design parameters chosen by the designer, $\iota > 0$ is a small constant to avoid singularity, and the initial value $\hat{b}(0) > 0$. The parameter estimation error is defined in the form of

$$\tilde{b} = b - e_{\min}\hat{b}, \tag{34}$$

which constitutes the second part of the overall Lyapunov candidate as

$$V_2 = \frac{1}{2\sigma e_{\min}}\tilde{b}^2. \tag{35}$$

We now present the following adaptive controller for the attitude tracking error dynamics defined in (7) to achieve attitude tracking despite actuator faults:

$$\boldsymbol{u}_c = -\left(k + \frac{\hat{b}\psi^2(\cdot)}{\psi(\cdot)\|\boldsymbol{\omega}_a\| + \iota}\right)\boldsymbol{\omega}_a, \tag{36}$$

where k is a positive design parameter.

Considering the composite Lyapunov candidate $V = V_1 + V_2$, it follows from (32) and (33) that

$$\begin{aligned}\dot{V} \leq & -\lambda\left(\alpha\omega_{e,\max} - \frac{\gamma}{2}\right)\boldsymbol{q}_e^T\boldsymbol{q}_e - \eta\boldsymbol{\omega}_f^T\boldsymbol{\omega}_f \\ & + b\psi(\cdot)\|\boldsymbol{\omega}_a\| + \boldsymbol{\omega}_a^T\boldsymbol{E}\boldsymbol{u}_c + \frac{c\alpha^2}{4g_2}\omega_{e,\max}^3 \\ & + \tilde{b}\left(\varrho\hat{b} - \frac{\psi^2(\cdot)\|\boldsymbol{\omega}_a\|^2}{\psi(\cdot)\|\boldsymbol{\omega}_a\| + \iota}\right)\end{aligned} \tag{37}$$

Then, substituting the control law $\boldsymbol{u}_c$ into the foregoing inequality yields

$$\begin{aligned}\dot{V} \leq & -\lambda\left(\alpha\omega_{e,\max} - \frac{\gamma}{2}\right)\boldsymbol{q}_e^T\boldsymbol{q}_e - ke_{\min}\boldsymbol{\omega}_a^T\boldsymbol{\omega}_a - \eta\boldsymbol{\omega}_f^T\boldsymbol{\omega}_f \\ & - \frac{\varrho}{2e_{\min}}\tilde{b}^2 + \frac{\varrho}{2e_{\min}}b^2 + b\iota + \frac{c\alpha^3}{4g_2}\omega_{e,\max}^3,\end{aligned} \tag{38}$$

where the fact $\tilde{b}\hat{b} \leq \frac{1}{2e_{\min}}(b^2 - \tilde{b}^2)$ is used. Since γ, g_1, g_2, and λ are small constants chosen arbitrarily for Lyapunov analysis, we can always select proper design parameters T_0, c, and α such that

$$\alpha\omega_{e,\max} - \frac{\gamma}{2} > 0, \tag{39}$$

$$\eta = \frac{1}{T_0} - \frac{c\alpha\omega_{e,\max}(g_1+g_2)}{4} - \frac{\lambda}{2\gamma} > 0. \tag{40}$$

Consequently, we obtain

$$\dot{V} \leq -\kappa V + \mu, \tag{41}$$

where two positive constants κ and μ are given by

$$\kappa = \min\left\{\alpha\omega_{e,\max} - \frac{\gamma}{2}, \frac{2ke_{\min}}{J_{\max}}, 2\eta, \sigma\varrho\right\}, \tag{42}$$

$$\mu = \frac{\varrho}{2e_{\min}}b^2 + b\iota + \frac{c\alpha^3}{4g_2}\omega_{e,\max}^3 + 4\lambda\left(\alpha\omega_{e,\max} - \frac{\gamma}{2}\right). \tag{43}$$

The above design procedure can be summarized in the following theorem, which contains the results of adaptive control for rigid-body attitude tracking systems.

Theorem 1: Considering the attitude tracking error system (7) with actuator faults and angular velocity constraints. Suppose that the design parameters T_0, c, and α are chosen to satisfy conditions (39) and (40). If the adaptive controller $\boldsymbol{u}_c$ is given by (36) and the update law is synthesised as (33), then the closed-loop system is uniformly ultimately bounded in the sense that all of the signals are bounded. Furthermore, the attitude tracking error $\boldsymbol{q}_e$, angular velocity tracking error $\boldsymbol{\omega}_e$, and virtual tracking error $\boldsymbol{\omega}_a$ converge to small invariant sets containing origin, that is, $\lim_{t\to\infty}\boldsymbol{q}_e(t) \in \Omega_{\boldsymbol{q}_e}$, $\lim_{t\to\infty}\boldsymbol{\omega}_e(t) \in \Omega_{\boldsymbol{\omega}_e}$, and $\lim_{t\to\infty}\boldsymbol{\omega}_a(t) \in \Omega_{\boldsymbol{\omega}_a}$.

Proof. From inequality (41), it can be shown that the closed-loop systems is uniformly ultimately bounded stable [31], and the signals $\boldsymbol{q}_e$, $\boldsymbol{\omega}_a$, $\boldsymbol{\omega}_f$, and $\tilde{b}$ are all bounded for all $t \geq 0$. Furthermore, according to (38), it is clear that $\dot{V} < 0$ if

$$\|\boldsymbol{q}_e\| > \sqrt{\frac{\phi}{\lambda\left(\alpha\omega_{e,\max} - \frac{\gamma}{2}\right)}}, \quad \texttt{or } \|\boldsymbol{\omega}_a\| > \sqrt{\frac{\phi}{ke_{\min}}}, \ \texttt{or } \|\boldsymbol{\omega}_f\| > \sqrt{\frac{\phi}{\eta}}, \tag{44}$$

where ϕ is a constant defined as $\phi = \frac{\varrho}{2e_{\min}}b^2 + b\iota + \frac{c\alpha^3}{4g_2}\omega_{e,\max}^3$. As a result, the decrease of $\dot{V}$ drives $\|\boldsymbol{q}_e\|$, $\|\boldsymbol{\omega}_a\|$, and $\|\boldsymbol{\omega}_f\|$ into $\|\boldsymbol{q}_e\| \leq \sqrt{\frac{\phi}{\lambda\left(\alpha\omega_{e,\max} - \frac{\gamma}{2}\right)}}$, $\|\boldsymbol{\omega}_a\| \leq \sqrt{\frac{\phi}{ke_{\min}}}$, and $\|\boldsymbol{\omega}_f\| \leq \sqrt{\frac{\phi}{\eta}}$, respectively. Moreover, it is clear from (15) and (16) that $\|\boldsymbol{\omega}_e\| \leq \|\omega_a\| + \|\boldsymbol{\omega}_f\| + \alpha\|\boldsymbol{\omega}_v^0\|$. From (12), we have $\|\boldsymbol{\omega}_v^0\| \leq c\omega_{e,\max}\|\boldsymbol{q}_e\|$ and thus $\|\boldsymbol{\omega}_e\| \leq \|\boldsymbol{\omega}_a\| + \|\boldsymbol{\omega}_f\| + \alpha c\omega_{e,\max}\|\boldsymbol{q}_e\|$. Therefore, it is obtained that the attitude tracking error, angular velocity tracking error, and virtual tracking error are uniformly ultimately bounded as $\lim_{t\to\infty}\boldsymbol{q}_e(t) \in \Omega_{\boldsymbol{q}_e}$, $\lim_{t\to\infty}\boldsymbol{\omega}_e(t) \in \Omega_{\boldsymbol{\omega}_e}$, and $\lim_{t\to\infty}\boldsymbol{\omega}_a(t) \in \Omega_{\boldsymbol{\omega}_a}$, where $\Omega_{\boldsymbol{q}_e}$, $\Omega_{\boldsymbol{\omega}_e}$, and $\Omega_{\boldsymbol{\omega}_a}$ are small invariant sets containing the origin defined as

$$\Omega_{\boldsymbol{q}_e} = \left\{ \boldsymbol{q}_e \middle| \|\boldsymbol{q}_e\| \leq \sqrt{\frac{\phi}{\lambda\left(\alpha\omega_{e,\max} - \frac{\gamma}{2}\right)}} \right\}, \tag{45}$$

$$\Omega_{\boldsymbol{\omega}_e} = \left\{ \boldsymbol{\omega}_e \middle| \|\boldsymbol{\omega}_e\| \leq \sqrt{\frac{\phi}{ke_{\min}}} + \sqrt{\frac{\phi}{\eta}} + \alpha c\omega_{e,\max}\sqrt{\frac{\phi}{\lambda\left(\alpha\omega_{e,\max} - \frac{\gamma}{2}\right)}} \right\}, \tag{46}$$

$$\Omega_{\boldsymbol{\omega}_a} = \left\{ \boldsymbol{\omega}_a \middle| \|\boldsymbol{\omega}_a\| \leq \sqrt{\frac{\phi}{ke_{\min}}} \right\}. \tag{47}$$

This completes the proof. □

Remark 2: Since the actuator effectiveness matrix $\boldsymbol{E}(\cdot)$ is not used in the controller, adaptive law, and command filter, the proposed control approach is able to achieve attitude tracking regardless of actuator health condition, i.e., in both fault-free and faulty situations. In addition, the proposed control scheme is independent of the physical inertia information, and thus it has a simple structure.

Remark 3: The safety scale α is used to provide a margin for the angular velocity to avoid reaching its maximal value. If we set its value to be 1, which means that there is no saturation margin, the angular velocity may exceeds this limitation due to the velocity tracking error under the proposed controller in Equation (37). However, if a conservative safety scale α is selected, the spacecraft may not reach the maximal slew rate and change its angular velocity slowly.

Remark 4: The implementation of the command filter-based controller (36) and adaptive law (33) requires values of the gains k, α, T_0, c, ϱ, and ι. The selecting principles for values of these design parameters are given in the following.

1) A larger k leads to a faster convergence rate and smaller steady-state error of $\boldsymbol{\omega}_a$ and $\boldsymbol{\omega}_e$ but a larger control torque adversely.
2) The value of the safety scale α in the command filter should be slightly smaller than 1, for example 0.95, which ensures that angular velocity is confined to its maximal limitation and a fast attitude maneuver is also achieved in the meantime.
3) The time constant T_0 in the command filter should be a small value to achieve a fast response of the command filter and satisfy the stability condition (40).
4) The parameter c in the command filter is chosen to be large enough to satisfy (14) of Property 1. However, a large c shall give rise to a large system steady-state error.
5) A smaller ϱ in the adaptive law may bring about a smaller steady-state error, but the convergence rate of $\hat{b}$ becomes slow if it is too small.
6) The parameter ι is used to smooth the controller and avoid singularity, so it is chosen to be a small constant.

IV. Simulations

Simulation results for a rigid spacecraft are presented in this section to illustrate the effectiveness of the command filter-based FTC scheme. The inertia matrix of the spacecraft is $\boldsymbol{J} = [20\ 1.2\ 0.9; 1.2\ 17\ 1.4; 0.9\ 1.4\ 15]$ kg $\cdot$ m^2 [32]. The external disturbances are assumed to $\boldsymbol{d} = 0.001 \times [\sin(0.8t)\ \cos(0.5t)\ \sin(0.2t)]^T$ Nm, which is larger than the maximal real disturbances in space environment. The initial attitude and angular velocity are set as $\boldsymbol{Q}(0) = [-0.5\ -0.3\ -0.4\ 0.7071]^T$ and $\boldsymbol{\omega}(0) = [0\ 0\ 0]^T$ rad/s, respectively. The desired attitude motion expressed in the body frame with respect to inertial frame is supposed to be

$$\boldsymbol{q}_d(t) = \left[\frac{1}{\sqrt{30}}\sin(-0.1t)\ \frac{1}{\sqrt{60}}\sin(-0.2t)\ 0.1\cos(-0.1t)\right]^T$$

and $q_{d0} = \sqrt{1 - \boldsymbol{q}_d^T\boldsymbol{q}_d}$. Using $\dot{\boldsymbol{q}}_d = \frac{1}{2}(\boldsymbol{q}_d^\times + q_{d0}\boldsymbol{I}_3)\boldsymbol{\omega}_d$ and $\dot{q}_{d0} = -\frac{1}{2}\boldsymbol{q}_d^T\boldsymbol{\omega}_d$, the desired angular velocity $\boldsymbol{\omega}_d$ can be obtained with a maximal value $\boldsymbol{\omega}_{d,\max} = 0.055$ rad/s. In the simulation, it is assumed that the slew rate of the rigid spacecraft is limited to 0.155 rad/s due to the saturation limit of low-rate gyro. Based on (10), this slew rate constraint is equivalent to the angular rate error constraint given as $|\omega_{e,i}(t)| \leq 0.1$ rad/s. We also assume that actuator generate a continuous control torque with a maximal output of 4 Nm.

For comparison purposes, the widely used cascade PD controller [21] and the proposed command filter-based control with adaptive gains as given in (36) and (33) are tested. The cascade PD controller is given by

$$\boldsymbol{u}_c = -\mathrm{sat}\left[\boldsymbol{J}(2k_p\mathrm{sat}(\boldsymbol{q}_e) + k_d\boldsymbol{\omega}_e)\right], \tag{48}$$

where the inner and outer saturation functions denoted as $\mathrm{sat}(\cdot)$ are used to limit the magnitude of angular rate error and commanded control torque, respectively. The control gains in (48) are chosen as $k_p = 4$ and $k_d = 3.64$. The parameters for the proposed controller in (36) are set as $k = 100$, $\alpha = 0.92$, $T_0 = 0.005$, $c = 80$, $\varrho = 10$, $\sigma = 0.1$, and $\iota = 0.005$. The initial value of $\hat{b}(t)$ in (33) is chosen as $\hat{b}(0) = 0.1$.

A. Response in the absence of actuator fault

In this case, we assume that all the actuators are fault free. Figs. 1 and 2 show the closed-loop system performance in the absence of actuator fault by using command filter-based attitude tracking controller and cascade PD controller, respectively. As seen in Fig. 1, the attitude and angular velocity tracking errors converge to a neighbourhood of the origin under the proposed attitude controller. It is noted from Figs. 1b and 1e that the magnitudes of angular velocity error and angular velocity are bounded within their pre-defined maximal values (0.1 rad/s and 0.155 rad/s, respectively), which verifies that the proposed control method has the capability to deal with angular rate constraint in attitude tracking maneuver. Fig. 1c illustrates the commanded control torque computed by the proposed controller. Although the commanded torque reaches saturation limit in the beginning of maneuver due to large tracking errors, the stability of the overall system is still maintained. Referring to Fig. 1d, the convergence of the virtual tracking error as illustrated in Theorem 1 is also verified. The adaptive parameter $\hat{b}(t)$ is shown in Fig. 1f, from which it is observed that $\hat{b}$ are bounded; thus, the efficacy of the proposed adaptation laws in (33) is demonstrated.

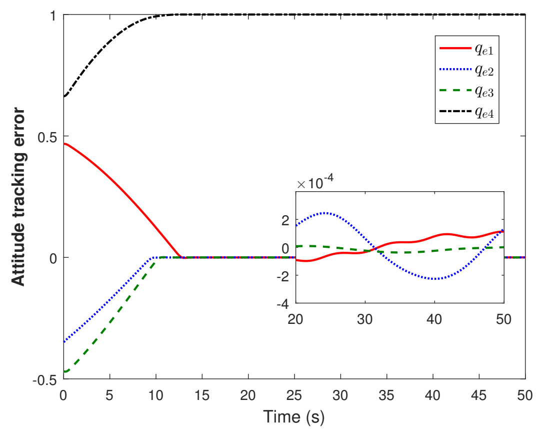

(a) Attitude tracking error.

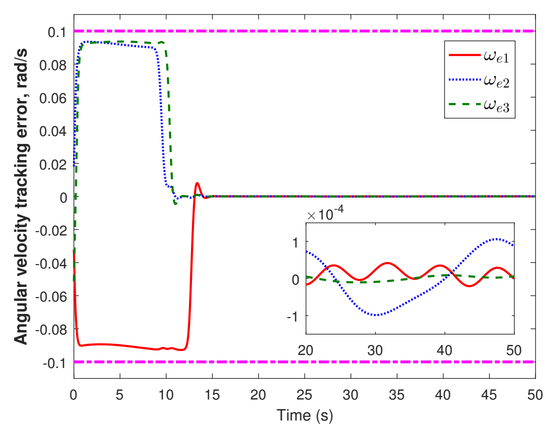

(b) Angular velocity tracking error.

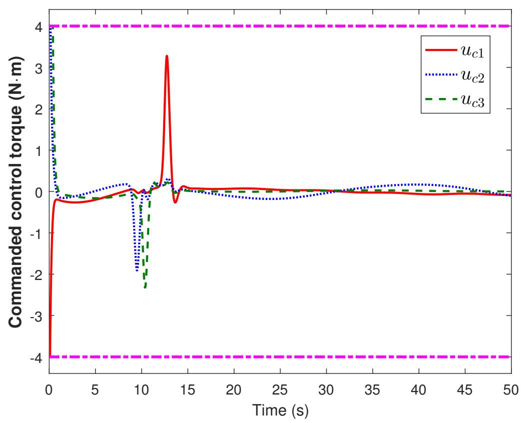

(c) Commanded control torque.

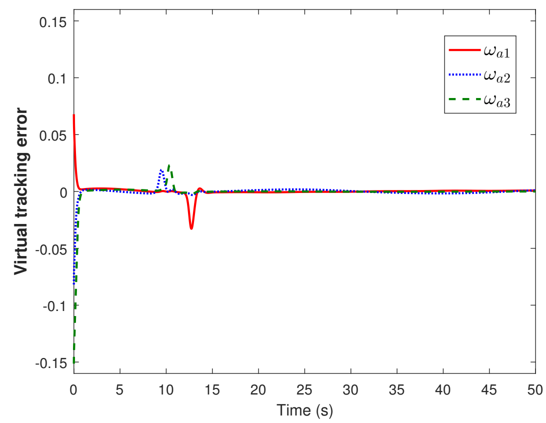

(d) Virtual tracking error.

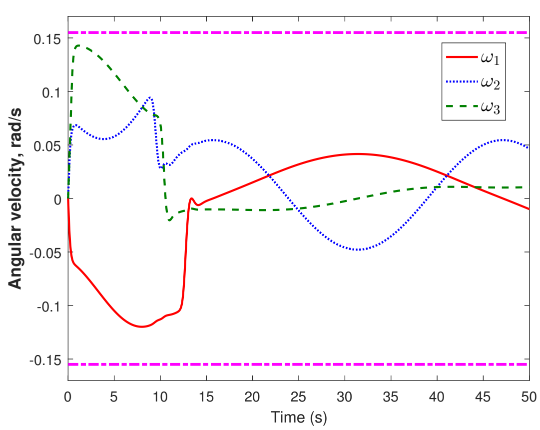

(e) Actual angular velocity.

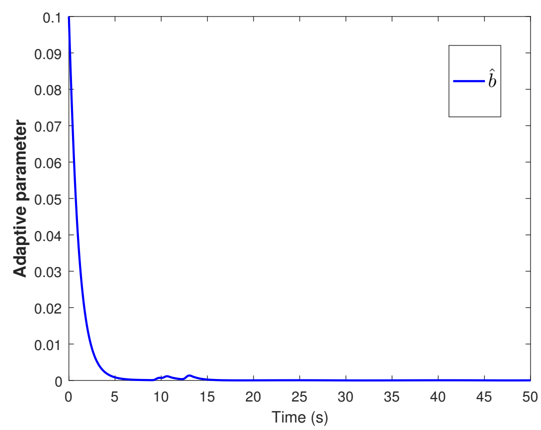

(f) Adaptive parameter $\hat{b}$.

Fig. 1. System performance using the proposed command filter-based controller in the absence of actuator fault .

Fig. 2 indicates that cascade PD controller can still stabilize the system in the fault-free case. However, as illustrated in Table I, the proposed controller in this paper achieves a better tracking performance than that of the cascade PD controller at almost the same overall energy consumption. Specifically, the command filter-based controller results in a steady-state attitude tracking error of 2.5×10^{-4} and angular velocity error of 1.1×10^{-4} rad/s, which are much smaller than that of the cascade PD controller (1.4×10^{-3} and 5.7×10^{-4} rad/s for attitude and angular velocity tracking errors, respectively). Here, it is noted that the angular velocity tracking error under the proposed method is always confined in its allowable maximum magnitude strictly, while the cascade PD controller could not ensure it.

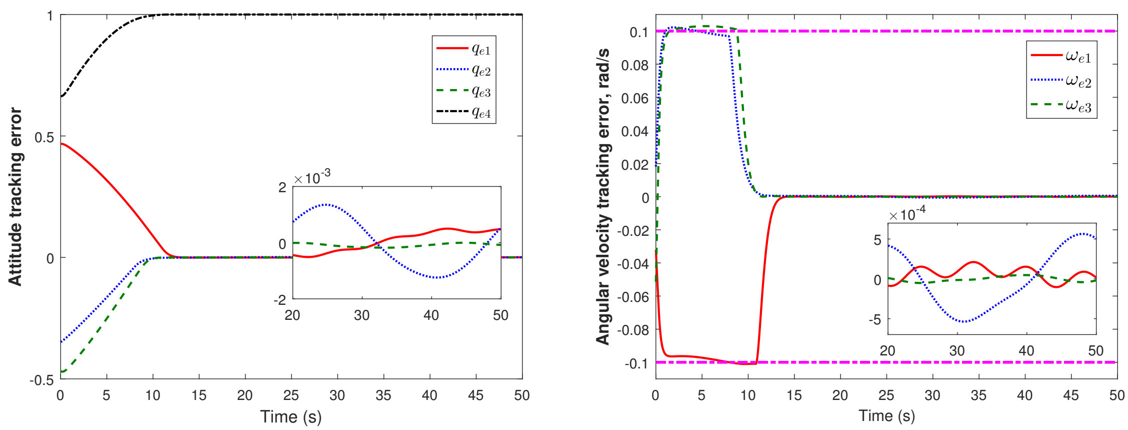

(a) Attitude tracking error. (b) Angular velocity tracking error.

Fig. 2. System performance using cascade PD controller in the absence of actuator fault .

TABLE I
COMPARISON OF CONTROL PERFORMANCE IN THE ABSENCE OF ACTUATOR FAULT

Controller	Control performance		
	SE[1] of $\boldsymbol{q}_e$	SE of $\boldsymbol{\omega}_e$	OCF[2]
Command filter-based FTC law in (36)	$\pm$ 2.5$\times 10^{-4}$	$\pm$ 1.1$\times 10^{-4}$	19.53
Cascade PD controller [21]	$\pm$ 1.4$\times 10^{-3}$	$\pm$ 5.7$\times 10^{-4}$	19.42

[1] SE stands for steady error.
[2] OCF denotes overall control effort defined as OCF $= \frac{1}{2}\int_0^T \|\boldsymbol{u}_c\|dt$, where T is the simulation time.

TABLE II
COMPARISON OF CONTROL PERFORMANCE IN THE PRESENCE OF ACTUATOR FAULT

Controller	Control performance		
	SE of $\boldsymbol{q}_e$	SE of $\boldsymbol{\omega}_e$	OCF
Command filter-based FTC law in (36)	$\pm$ 3.2$\times 10^{-3}$	$\pm$ 6.5$\times 10^{-4}$	207.80
Cascade PD controller [21]	$\pm$ 1.8$\times 10^{-2}$	$\pm$ 4.0$\times 10^{-3}$	205.86

B. Response in the presence of actuator fault

We now consider the case wherein the fault occurs in actuators during the attitude maneuver. Since only three actuators are used for attitude control, total failure on actuator is not taken into account. At $t = 5$ s, each actuator suffers from a partial loss of effectiveness fault, while at $t = 10$ s, these actuators also undergo a time-varying bias fault that enters the spacecraft dynamics in an additive way. The loss of effectiveness fault is described as

$$e_1(t) = \begin{cases} 1, & \text{if } t < 5 \\ 0.5 + 0.09\sin(0.05t) + 0.005\,\text{rand}(\cdot), & \text{if } t \geq 5 \end{cases}$$
$$e_2(t) = \begin{cases} 1, & \text{if } t < 5 \\ 0.6 + 0.10\cos(0.08t) + 0.008\,\text{rand}(\cdot), & \text{if } t \geq 5 \end{cases}$$
$$e_3(t) = \begin{cases} 1, & \text{if } t < 5 \\ 0.4 + 0.08\sin(0.06t) + 0.005\,\text{rand}(\cdot), & \text{if } t \geq 5 \end{cases}$$

while the additive bias fault is given by

$$f_{a1}(t) = \begin{cases} 0, & \text{if } t < 10 \\ 0.75 + 0.25\sin(0.04t), & \text{if } t \geq 10 \end{cases}$$
$$f_{a2}(t) = \begin{cases} 0, & \text{if } t < 10 \\ 0.95 + 0.05\sin(0.08t), & \text{if } t \geq 10 \end{cases}$$
$$f_{a3}(t) = \begin{cases} 0, & \text{if } t < 10 \\ 0.85 + 0.15\sin(0.06t), & \text{if } t \geq 10. \end{cases}$$

The function rand$(\cdot)$ generates a random value from the normal distribution with mean 0 and standard deviation 1.

In the presence of actuator fault, the system performance with the application of the proposed command filter-based controller (36) and the adaptive law (33) is demonstrated in Fig. 3. It is clear that the attitude tracking error and angular velocity tracking error are stabilized ultimately to a small compact set containing the origin. As observed in Figs. 3e and 3b, the angular velocity and its tracking error under the proposed controller are smaller than the corresponding maximal magnitudes strictly despite actuator faults. Fig. 3c depicts the time history of the commanded control torque. It is clear that the torque generated by the proposed controller compensates the effects of actuator faults and enhances the reliability of the attitude control systems. The real actuator output torque is shown in Fig. 3f, which demonstrates that actuator faults have affected the torque computed by the controller obviously. Although cascade PD controller can still stabilize the closed-loop systems with a slight less total control efforts, the control performance degrades dramatically with a steady-state attitude tracking error of 1.8$\times 10^{-2}$ and angular velocity tracking error of 4.0$\times 10^{-3}$ rad/s, which are about one order larger than that using the proposed controller. The detailed control performance comparison under two controllers for the attitude tracking system in the presence actuator faults can be found in Table II. Similar to the previous case, it is also noted that the cascade PD controller cannot ensure the angular velocity tracking error constraints strictly.

In addition, in both fault-free and faulty actuator cases, it is observed from Figs. 1d and 3d that there exists a sudden increase in the virtual tracking error. The reason for this

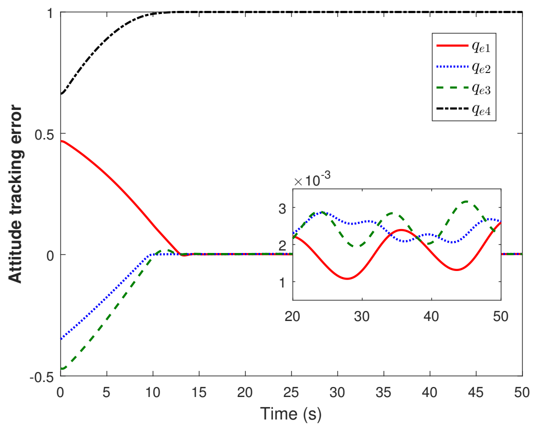

(a) Attitude tracking error.

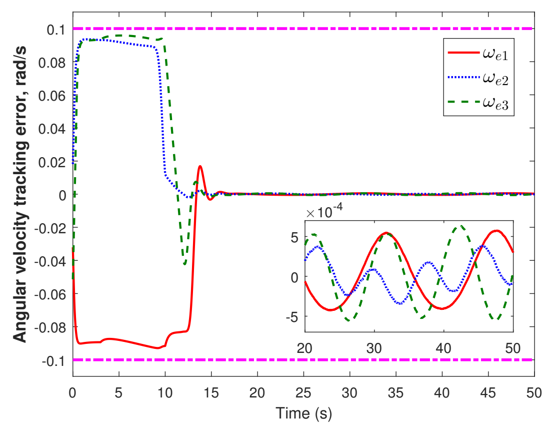

(b) Angular velocity tracking error.

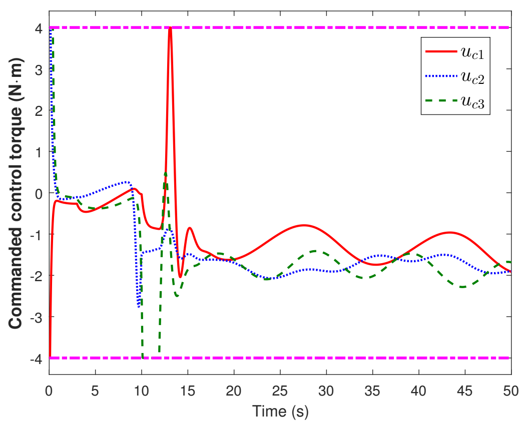

(c) Commanded control torque.

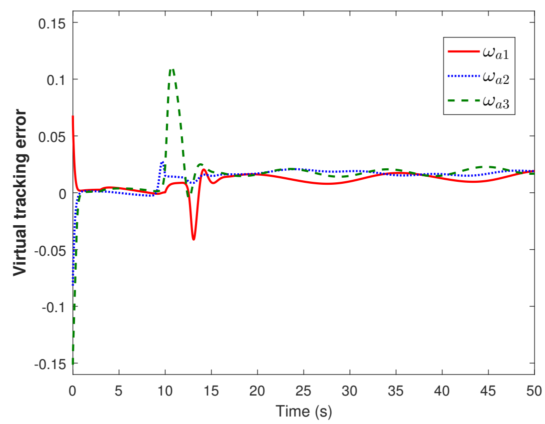

(d) Virtual tracking error.

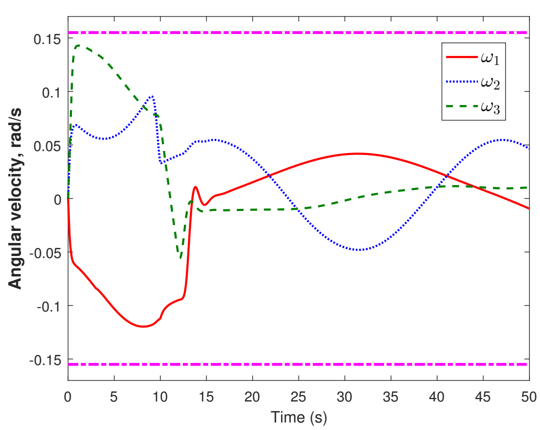

(e) Actual angular velocity.

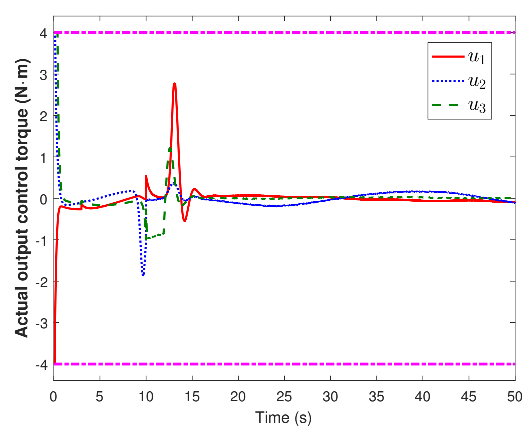

(f) Actual output torque $\boldsymbol{u}$.

Fig. 3. System performance using the proposed command filter-based controller in the presence of actuator fault .

phenomenon is that the virtual angular velocity tracking error command $\boldsymbol{\omega}_v$ has a sudden jump when the quaternion tracking error becomes small. As the virtual tracking error $\boldsymbol{\omega}_a$ describes the discrepancy between angular velocity tracking error and its virtual command produced by command filter and converges to zero when $t \to \infty$, the virtual tracking error $\boldsymbol{\omega}_a$ also experience a sudden change if there exist a sudden change of the virtual command $\boldsymbol{\omega}_v$. Based on the property of hyperbolic function used in Equation (13), a rapid change of the input of the command filter occurs when the attitude tracking error reaches a small value. Since the virtual command $\boldsymbol{\omega}_v$ follows its input $\boldsymbol{\omega}_v^0$, it is clear that $\boldsymbol{\omega}_v$ experience a rapid change when the attitude tracking error converge to a small value. Therefore, it is reasonable that the virtual tracking error experience a

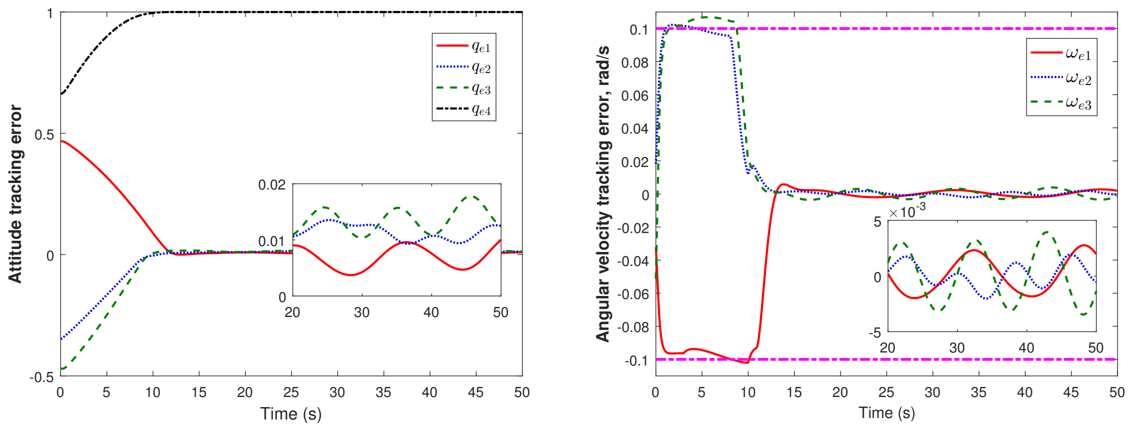

(a) Attitude tracking error.

(b) Angular velocity tracking error.

Fig. 4. System performance using cascade PD controller in the presence of actuator fault .

sudden increase when the attitude tracking error converges to a small value. Moreover, it is observed from the Tables I and II that the overall control efforts in presence of actuator faults is much larger than that in the fault-free case. The reason for this large difference is that extra control efforts are spent for compensating the fault effects, especially after the occurrence of the bias fault.

V. Conclusions

This paper addresses the problem of FTC design for rigid-body attitude tracking control in the presence of actuator faults and angular velocity constraints. Aided by a command filter that constructs a virtual angular velocity with bounded magnitude, the angular velocity error is restricted to a certain range determined by the safety scale and angular rate constraint. Consequently, an command filter-based adaptive controller without utilizing the fault information is proposed such that the attitude and angular velocity tracking errors converge to a compact set containing the origin ultimately in both faulty and fault-free cases. Finally, the effectiveness of the proposed strategy are illustrated in simulation. Through simulation results, it is observed that the proposed controller has the capability to handle actuator faults and angular rate constraints while achieving three-axis attitude tracking.

References

[1] W. Luo, Y.-C. Chu, and K.-V. Ling, "Inverse optimal adaptive control for attitude tracking of spacecraft," *IEEE Transactions on Automatic Control*, vol. 50, no. 11, pp. 1639–1654, Nov. 2005.

[2] J. D. Boskovic, S. Li, and R. K. Mehra, "Robust tracking control design for spacecraft under control input saturation," *Journal of Guidance, Control, and Dynamics*, vol. 27, no. 4, pp. 627–633, Jan.-Feb. 2004.

[3] A. M. Zanchettin, A. Calloni, and M. Lovera, "Robust magnetic attitude control of satellites," *IEEE/ASME Transactions on Mechatronics*, vol. 18, no. 4, pp. 1259–1268, Aug 2013.

[4] C. G. Mayhew, R. G. Sanfelice, and A. R. Teel, "Quaternion-based hybrid control for robust global attitude tracking," *IEEE Transactions on Automatic Control*, vol. 56, no. 11, pp. 2555–2566, Nov. 2011.

[5] A. Tayebi, "Unit quaternion-based output feedback for the attitude tracking problem," *IEEE Transactions on Automatic Control*, vol. 53, no. 6, pp. 1516–1520, Jul. 2008.

[6] C. Edwards and Y. Shtessel, "Adaptive continuous higher order sliding mode control," *Automatica*, vol. 65, pp. 183–190, Mar. 2016.

[7] D. Y. Negrete-Chvez and J. A. Moreno, "Second-order sliding mode output feedback controller with adaptation," *International Journal of Adaptive Control and Signal Processing*, vol. 30, p. 15231543, 2016.

[8] H. Alwi and C. Edwards, "Fault tolerant control using sliding modes with on-line control allocation," *Automatica*, vol. 44, no. 7, pp. 1859–1866, Jul. 2008.

[9] H. Alwi, C. Edwards, and C. P. Tan, *Fault detection and fault-tolerant control using sliding modes*. Berlin, Germany: Springer, 2011.

[10] X. Yu, P. Li, and Y. M. Zhang, "Fault-tolerant aircraft control based on self-constructing fuzzy neural networks and multivariable smc under actuator faults," *IEEE Transactions on Fuzzy Systems*, 2017, online available.

[11] X. Yu, Y. Fu, P. Li, and Y. M. Zhang, "The design of fixed-time observer and finite-time fault-tolerant control for hypersonic gliding vehicles," *IEEE Transactions on Industrial Electronics*, vol. 65, no. 5, pp. 4125–4144, May 2018.

[12] Y. M. Zhang and J. Jiang, "Bibliographical review on reconfigurable fault-tolerant control systems," *Annual Reviews in Control*, vol. 32, no. 2, pp. 229–252, Dec. 2008.

[13] X. Yu, Y. Fu, and Y. M. Zhang, "Aircraft fault accommodation with consideration of actuator control authority and gyro availability," *IEEE Transactions on Control Systems Technology*, 2017, online available.

[14] S. Yin, B. Xiao, S. X. Ding, and D. Zhou, "A review on recent development of spacecraft attitude fault tolerant control system," *IEEE Transactions on Industrial Electronics*, vol. 63, no. 5, pp. 3311–3320, May 2016.

[15] W. C. Cai, X. H. Liao, and Y. D. Song, "Indirect robust adaptive fault-tolerant control for attitude tracking of spacecraft," *Journal of Guidance, Control, and Dynamics*, vol. 31, no. 5, pp. 1456–1463, Sep.-Oct. 2008.

[16] D. Bustan, S. K. H. Sani, and N. Pariz, "Adaptive fault-tolerant spacecraft attitude control design with transient response control," *IEEE/ASME Transactions on Mechatronics*, vol. 19, no. 4, pp. 1404–1411, Aug. 2014.

[17] Q. Shen, D. Wang, S. Zhu, and K. Poh, "Finite-time fault-tolerant attitude stabilization for spacecraft with actuator saturation," *IEEE Transactions on Aerospace and Electronic Systems*, vol. 51, no. 3, pp. 2390–2405, 2015.

[18] B. Xiao, M. Huo, X. Yang, and Y. Zhang, "Fault-tolerant attitude stabilization for satellites without rate sensor," *IEEE Transactions on Industrial Electronics*, vol. 62, no. 11, pp. 7191–7202, Nov. 2015.

[19] C. C. Chen, S. S. D. Xu, and Y. W. Liang, "Study of nonlinear integral sliding mode fault-tolerant control," *IEEE/ASME Transactions on Mechatronics*, vol. 21, no. 2, pp. 1160–1168, April 2016.

[20] S. Zhu, D. Wang, Q. Shen, and E. K. Poh, "Satellite attitude stabilization control with actuator faults," *Journal of Guidance, Control, and Dynamics*, 2017, online available.

[21] B. Wie, D. Barley, and H. C., "Rapid multitarget acquisition and pointing control of agile spacecraft," *Journal Guidance, Control, and Dynamics*, vol. 25, no. 1, pp. 96–104, Jan.-Feb. 2002.

[22] Q. Hu, "Robust adaptive backstepping attitude and vibration control with L_2-gain performance for flexible spacecraft under angular velocity constraint," *Journal of Sound and Vibration*, vol. 327, no. 3, pp. 285–298, 2009.

[23] X. Cao, C. Yue, M. Liu, and B. Wu, "Time efficient spacecraft maneuver using constrained torque distribution," *Acta Astronautica*, vol. 123, pp. 320–329, Jun.-Jul. 2016.

[24] M. Li, M. Hou, and C. Yin, "Adaptive attitude stabilization control design for spacecraft under physical limitations," *Journal of Guidance, Control, and Dynamics*, vol. 39, no. 9, pp. 2179–2183, Sep. 2016.

[25] M. J. Sidi, *Spacecraft Dynamics and Control*. Cambridge, U.K.: Cambridge, NY: Cambridge University Press, 1997.

[26] J. T. Y. Wen and K. Kreutz-Delgado, "The attitude control problem," *IEEE Transactions on Automatic Control*, vol. 36, no. 10, pp. 1148–1162, Oct. 1991.

[27] Q. Shen, D. Wang, S. Zhu, and E. K. Poh, "Integral-type sliding mode fault-tolerant control for attitude stabilization of spacecraft," *IEEE Transactions on Control Systems Technology*, vol. 23, no. 3, pp. 1131–1138, 2015.

[28] ——, "Robust control allocation for spacecraft attitude tracking under actuator faults," *IEEE Transactions on Control Systems Technology*, vol. 25, no. 3, pp. 1068–1075, 2017.

[29] B. Wie, *Space Vehicle Dynamics and Control*. AIAA, Reston, VA: AIAA Education Series, 2008.

[30] B. T. Costic, D. M. Dawson, M. S. Queiroz, and V. Kapila, "Quaternion-based adaptive attitude tracking controller without velocity measurements," *Journal of Guidance, Control, and Dynamics*, vol. 24, no. 6, pp. 1214–1222, Nov.-Dec. 2001.

[31] H. K. Khalil, *Nonlinear Systems*, 2nd ed. Prentice-Hall, Upper Saddle, River, NJ, 2002.

[32] Q. Shen, D. Wang, S. Zhu, and E. K. Poh, "Inertia-free fault-tolerant spacecraft attitude tracking using control allocation," *Automatica*, vol. 62, pp. 114–121, Dec. 2015.

Qiang Shen (S'12-M'16) received his B.E. degree in automation from the Northwestern Polytechnical University, Xian, China, in 2010 and the Ph.D degree from Nanyang Technological University, Singapore, in 2016. From 2015 to 2016, he held an Associate Scientist position at Temasek Laboratories, National University of Singapore, Singapore, and then a Research Scientist position at the same Laboratories from 2016 to 2017. He is currently a Postdoctoral Research Associate with the School for Engineering of Matter, Transport and Energy, Arizona State University, Tempe, AZ, USA. His research interests include active model discrimination, fault tolerant control, and control allocation.

Chengfei Yue (S'16) received a B.Eng. degree in Flight Vehicle Design and Engineering from Honor School, Harbin Institute of Technology, Harbin, P.R.C in 2013. From Sep. 2017 to Dec. 2017, he was a visiting PhD student at Ryerson University, Canada. He is currently pursuing a Ph.D. degree with the Department of Electrical and Computer Engineering, National University of Singapore, Singapore. His current research interests include underactuated attitude control of spacecraft, fault-tolerant control system, modelling and simulation using control moment gyros and adaptive control.

Cher Hiang Goh (SM'11) received his Diplom-Ingeneur (M.Sc.) and Doktor-Ingenieur (Ph.D) Degrees from Universitaet Paderborn (Germany) and Ruhr-Boechum Universitaet (Germany) in 1983 and 1993 respectively, while under government scholarship. He is currently a Distinguished Member of Technical Staff of DSO National Laboratories. He is also an Adjunct Professor to National University of Singapore (NUS). He is the director of Singapore 1st Micro-satellite project (X-Sat) and led a team of about 50 engineers to successfully design, develop and launch the micro-satellite in 2011. He was a Distinguished Visiting Professor to Naval Postgraduate School of U.S.A. in 2012. From 2013 to 2016, he was seconded to National University of Singapore. There he led the space systems R&Ds as projects Principal Investigator and also the Director of the Satellite and Airborne Radar Systems Laboratory (SARSL). In DSO, he held various positions such as Programme Manager and Research Head (Guidance & Control Laboratory). He chaired the 1st Singapore Space Symposium in 2014 and is also General Co-Chair of IEEE Asia Pacific Synthetic Aperture

Baolin Wu received his B. Eng and M. Eng degrees in spacecraft design from the Harbin Institute of Technology, Harbin, China, in 2003 and 2005, respectively, and the Ph.D. degree in spacecraft formation control from Nanyang Technological University, Singapore, in 2011. He spent two years in the satellite R&D industry. He developed algorithms for attitude determination and control. Since 2014, he has been working on academic research as associate professor at Research Center of Satellite Technology, Harbin Institute of Technology, Harbin, China. His current research area is in spacecraft attitude control, attitude synchronization, spacecraft formation control, and trajectory optimization.

Danwei Wang (S'88-M'89-SM'04) received his Ph.D and MSE degrees from the University of Michigan, Ann Arbor in 1989 and 1984, respectively. He received his B.E degree from the South China University of Technology, China in 1982. He is professor in the School of Electrical and Electronic Engineering, Nanyang Technological University, Singapore. He is director of the STE-NTU Corp Lab, NTU. He has served as head, Division of Control and Instrumentation from 2005 to 2011 and director of the Centre for Centre for System Intelligence and Efficiency until 2016. He also served as general chairman, technical chairman and various positions in international conferences. He has served as an associate editor of Conference Editorial Board, IEEE Control Systems Society. He is an associate editor of International Journal of Humanoid Robotics and invited guest editor of various international journals. He was a recipient of Alexander von Humboldt fellowship, Germany. He has